

Drone Application for Micro Basin and Flow Identification on Hilly Area, UNNES, Central Java

Fahrudin Hanafi¹, Sigit Bayhu Iryanthony²
{fahrudin.hanafi@mail.unnes.ac.id¹, sigitbayhuiryAnthony@gmail.com²}

¹Universitas Negeri Semarang, Indonesia

²Universitas Diponegoro, Indonesia

Abstract. Reliable topographic data needs as input for earth studies. Drone has the potential as a reliable source for detailed scale, if controlled with accurate GCP. UNNES has a topography with a representative sudden slope configuration to test the quality of the data recording. This research objectives are knowing drones potential in the detailed mapping of the 3D micro basin or flow data. Validate and comparing with DEMNAS, terrestrial RTK, for identifying basin areas or flow in the UNNES. Data acquisition using P3 Pro DJI Drone, capture PIX4D mapping software, recorded below 100 m altitudes, overlay 80%, and single grid mission. Research result showed that drones have the ability as a topographic data source by carrying out certain requirements such as a representative GCP, good quality photos and low altitude. Drone data has the flexibility on the spatial resolution and all the characteristics needed for micro DSM, morphometric and hydrological analysis. This research using RMSH 2.5 cm, 5.1 cm RMSV, and 0.98 m average accuracy.

Keywords: Drone Application, Micro Basin, Flow.

1. Introduction

Unmanned aerial vehicles (UAVs), or so-called drones, unmanned aerial systems (UAS), and the pilotless aircraft (RPA) is a vehicle remotely fly the aerodynamic principles to rely on the ability of control without a pilot or autonomous [1]. The early development of UAV used for military purposes around the 19th Century [2]. Ease of use and affordable price make the drones now often used as a reliable instrument in a variety of disciplines. Because of its flexibility, reach and profits in a tough area with security and safety of humans [2]. UAV technology over satellite images and aerial photography plain has the advantage of a low altitude, very high spatial resolution, high-return period of shooting, and low cost [3]. UAV technology becomes cheaper over time, thus experiencing a significant increase in sales [4] drone technology. The rapid development in recent decades [5]. Applied drones in various mapping is quite varied as in the field of disaster vulnerability [5], Agricultural plantation [6], asset archaeological / heritage [7], and mining [8].

Environmental problems such as sediment, flooding, and sediment increasingly complex, as well as the modeling techniques. The paradigm in decision making based on administrative

boundaries for environmental management is not relevant at this time, and now uses catchment or watershed based. Associated with the integrated watershed management [9], watershed spatial modeling depends on scale and cell size that is represented in the form of topography or flow pattern. Study of flow patterns, morpho topography and flow direction is an important topic in environmental sciences. For consideration, spatial variability is an important component of the study flow generation, both in the field and in the computer [10]. Modeling with topographic analysis has been done [11] for a small catchment area (microtopography). DEM watershed modeling (topography) is the main component that must be fulfilled availability [12] [13], because of practice for detail measurements on locations research are very limited. Using UAV data has the potential to identify flow patterns and stream generation, so measurements can be concentrated in prior area [14]. Identify the broad catchment scale can be met with a 30-meter resolution DEM data but the scale of detail not possible with 30-meter DEM [15], but the detail scale not possible with 30-meter [13] [7], because DEM data 30 m, dividing the territory into a few pixels that make some GIS algorithms are not work [14]. Detailed mapping of catchment areas can be done with the terrestrial laser scanning (TLS), or total station to produce high-precision terrain models [16]. Use of the terrestrial survey technology requires a lot of time[17], with LIDAR are costly [18], and the development of LIDAR drones is very expensive LIDAR [19] [2].

For the purposes of the investigation on land use UAV acquisition makes it possible to obtain data of high detailed morphologies of the area, which can be processed to DSM, which is close to the results of Lidar [20]. DEM results of the drones can, in many cases using to renew the old map data that do not cover the scope of the detail [7]. 3D information about the earth's surface processed through photogrammetric cloud data with several approaches and algorithms filtering [21][22][7]. DEM is very useful, without interference by vegetation cover and buildings [5][2].

Remote sensing data and GIS tools have the ability to generate the flow, direction, drainage of a catchment [23]. Raster data of elevation models can be automatically used as hydrologic input analysis, and catchment characteristics extraction such as network channel, slope, length of slope, sub-catchments, soil erosion or flood simulation [24]. DSM raster data is converted into a drone DTM, as data input in GIS that allows to calculate the difference of pixels value (height) in a matrix. This means that the height difference of a field DTM can be simulated as the flow direction. Determination of flow direction each pixels according to D8 algorithm are comparing the relative heights pixels to 8 pixels surrounding [25]. Flow Directions accumulate in a cell elevation models represent the amount of water flow direction which gathered in a basin[24]. The limit or threshold of flow accumulation can be assumed as the flow on downstream of real world. D8 algorithm commonly used in hydrologic research using ArcGIS platform and raster-based iteration process.

This study aims to determine the potential of low altitude drones for high-resolution mapping of micro-topography on hilly region which less than 100 hectares in UNNES (Universitas Negeri Semarang), Central Java Province. The mapping necessity of UNNES, cause since 1991 has undergone a development that affects land cover changes in the surrounding area. Landuse changes significantly grown 16% in less than 15 years[26]. UNNES located in upstream of Garang watershed, and layed on southern part of Mount Ungaran. Topography characteristics are hilly at of 200 meters above sea level. UNNES region is in Kaligetas geological formation with material breccia, tuff lava and smooth [27] so the radar data is not able to detect micro-topographic with a spatial resolution of less than 30 m².

2. Method

This study uses geodetic GPS Sokkia GRX 2, and the DJI Phantom Drone Advance 3 as the main data source. Direct Geo-referencing (Bench Mark) using geodetic GPS Sokkia GRX 2, with static methods for high accuracy [28]. A static method are postprocessing analysis to determine the absolute coordinates of BM through two reference locations oriented transversely to each other. Each point placed at an open location and recorded at least 45 minutes [29]. This study uses an Indonesia geodetic networks Benchmark (0 order) which ellipsoid reference managed by BIG, with UTM coordinates 434.778 mE, 9.228.005 mN, and elevation 31.17 msl. Flight path using 11 GCP (Ground Control Point) reference which has lower order (2nd order), which derived using static methods through Benchmark on Social Science Faculty of UNNES at coordinates 433.364 mE, 9.220.795 mN, and elevation 192,219 msl within 7.5 Km of 0 order benchmark. Derivation scheme order of 0 to 1st, and 1st to 2nd (drone control point) described in **Fig. 1**.

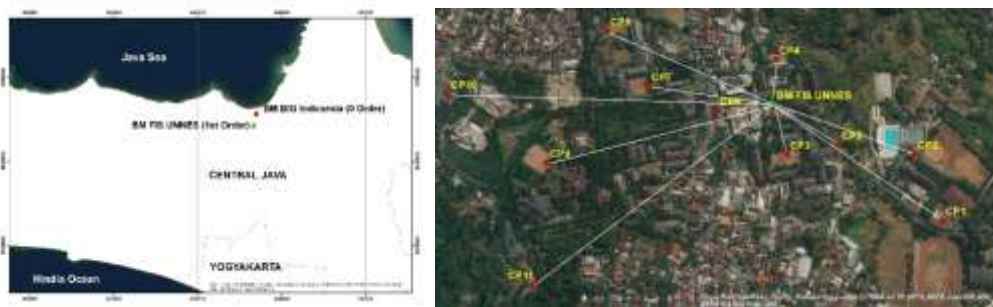


Fig. 1. GCP Ellipsoid to FIS UNNES (Left), BM FIS UNNES to Drone CP (Right).

RTK (Real-Time Kinematic) Methods used to accuracy test of elevation models which derived from the aerial drone record on low altitude. Photo acquisition using drones in automatically mode with PIX4D software, total taken on 7 times to flight at a 80 m altitude, with an area about 130 ha. Photo acquisition using drones on 85 m altitude has been done in Switzerland with static GCP-GNSS and RTK test to obtain vertical and horizontal accuracy o less than 0.02 m [28]. Each flight path used in study refers to any GCP spread evenly throughout the region, and have a vertical-horizontal RMS less than 5 cm. Micro-topographic mapping using low altitude aerial photography at a small research area (1 ha) has done at Windmill Island, Iceland getting resolution DSM of 2 cm. The DSM can define the flow direction and upstream of the snow through the catchment with a correlation (R^2) from 0.44 to 0.57 [30].

Field data acquisition process is determined with an autonomous flight path plan using a low-cost drone (DJI), remain the width of the study area. Aerial photos obtained is processed to give a high-resolution ortho imagery, DSM and DTM [4] [21] [6]. Furthermore, geographic location, size, and catchment on three-dimensional (3D) form, will be measured using orthoimage georeferencing, and DTM [7]. The results accuracy will be validated by comparing with pre-installed ground control point coordinates [5].

DSM derivatization level accuracy evaluated using a point to point, and grid to grid. Point to point method was evaluated by calculating the horizontal and vertical RMS between the RTK results, and DSM data point (DSM UAV, and DEMNAS). Grid method to compare the elevation raster value on the same grid, the RTK method were interpolated to get grid form

on the DSM. This is necessary because point to point do not represent the true topography, so DEM are accurate to represents topography or in 3-dimensional coordinates [31]. Interpolation grid size according to the radar image DEMNAS size which issued by BIG Indonesia. DEMNAS spatial resolution is 0:27-arcseconds, with vertical datum EGM 2008. DEMNAS is derived from the method of mass point adding/ data assimilation into the Digital Surface Model (IFSAR, TERASAR-X or ALOS-PALSAR) using the tension-surface GMT 0:32.

The final goal of this study was to examine the output of UAV DSM to determine and the potential to generate flow accumulation UNNES area. Accumulated flow are prepared using the D8 algorithm. D8 algorithm is matrix-based processing with Flow Direction and flow accumulation output in the form of pixels (grid) in integer format whose value ranges between 1 and 255. D8 algorithm is suitable for a small area with varied and high relief, but the precision level of DEM should not be lower than the gradient slope[32]. D8 algorithm output quality is dependent on the number of flat area pixels because of the discontinuous flow [32], and the number of sinks or centre cell with a lower value than other eight cell, also DEM accuracy on spatial resolution.

3. Result and Discussion

The derivatation SRGI Benchmark – (FIS) Social Science Faculty Benchmark - GCP flight plan using static method GPS which recorded in different duration. SRGI Benchmark to FIS Benchmark for 4 hours, and FIS Benchmark - GCP for 1-1.5 hours with varying results. Variation data recording caused by many aspects such as satellite clock, ephemeris error, receiver, ionospheric, tropospheric, and multipath [33].

Table.1. Static Analysis Method on SRGI BM - BM FIS UNNES - CP

GPS Observations					
<i>name</i>	<i>dN (m)</i>	<i>dE (m)</i>	<i>DHT (m)</i>	<i>Horz RMS (m)</i>	<i>Vert RMS (m)</i>
BASE 1 FIS-BM SRGI_	59 931	-113 074	9566	0003	0008
<i>name</i>	<i>grid N (M)</i>	<i>grid E (M)</i>	<i>Elevation</i>	<i>Horz RMS (m)</i>	<i>Vert RMS (m)</i>
Base FIS 1-CP1	9,220,522.554	433,763.869	193.071	.150	0.063
Base FIS 1-CP2	9,220,677.672	433,697.719	192.302	0,049	0,011
Base FIS 1-CP3	9,220,677.310	433,396.217	192.057	0,042	0.162
Base FIS 1-CP4	9,220,901.161	433,370.878	187.481	.309	0.261
Base FIS 1-CP5	9,220,699.518	433,517.911	191.715	0,006	0,017
Base FIS 1-CP6	9,220,780.175	433,231.324	189.158	0.007	0,011
Base FIS 1-CP7	9,220,837.504	433,069.944	189.216	0,005	0,012
Base FIS 1-CP8	9,220,968.072	432,973.504	192.212	0.007	.058
Base FIS 1-CP9	9,220,657.568	432,830.526	198.607	0,072	0.086
Base FIS 1-CP10	9,220,819.378	432,597.411	198.605	0.136	0.194
Base FIS 1-CP11	9,220,371.608	432,801.669	198.680	0.009	0.051
Average All				0072	0084
Average CP 2,3,5,6,7,8,9,11				0025	0051

GCP functions is providing XYZ location control of each photo on the guidelines set point. This will help improve the correction accuracy rather relying drones GPS and

comparison pixel shooting results. **Table.1.** shows that in 11 GCP total with average horizontal RMS 7.2 cm and 8.4 cm, but the research using the GCP with error rate less than 10 cm. The Averaging is a first error rate control and most simple [33]. To improve the data accuracy, the GCP 1, 4, and 10 are not used to obtain the average RMS horizontal vertical 2.5 cm and 5.1 cm. Thus the spatial resolution target of 2 cm as the derivate output DSM [30] with RMSE of 4.4 cm can be accomplish.

DTM is a digital model of the topography without land cover, while DSM contains elevation information including land cover and other features [34]. DTM in the photogrammetry through digital processes and algorithms to the eliminate elevation data of land cover. In terms of the accuracy, DTM which constructed from a mass point and breakline has good accuracy for the contour lines creation on the map. The making of DSM using the PIX4D software which similar to Agisoft software on 3D model creation process. Stages of data procession are from raw data (aerial photographs), creating the 3D point clouds, then 3D mesh triangulation process, to be produced DSM [35]. In this process include adjustment and control of alignment photograph, camera calibration, or conditional setting that can affect the results quality.

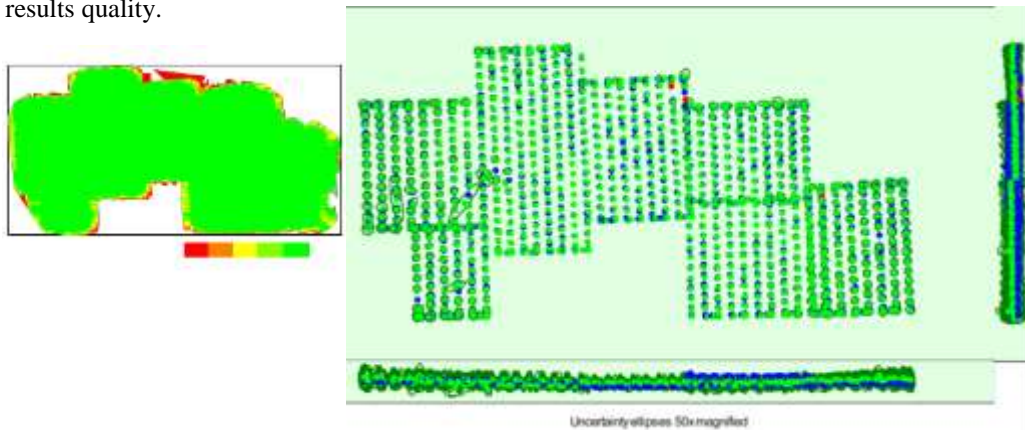


Fig. 2. Overlap (left), Computational Results Image / GCP and ties Manual position (right).

Fig.2. showed GCP computing quality of the photo around flight plan. Red color indicates unused / fail calibrated, dark green color indicates the absolute location quality with a small error. Results (**Fig.2, right**) shows the GCP quality and acquisition conditions qualify for the DSM high quality creation, with a low drone lens angle interference (ω : 0.08° ; ϕ : 0.05° ; and κ : 0.021°) or only requires a 2.7% internal parameter optimization so that the number of photos calibrated are 1078 of 1081 or 99.72%. Total overlap distribution of the entire study area also adequate (**Fig.2, left**) as indicated by the green color evenly across the study area, with red dot on the outside of the recorded area.

DEM data derived from aerial photography results then compared with the quality and accuracy of DEMNAS raster data (radar) based on point to point, and grid to grid. Pictures (**Fig.3**) shows the difference in results between DEMNAS and DEM acquisition.

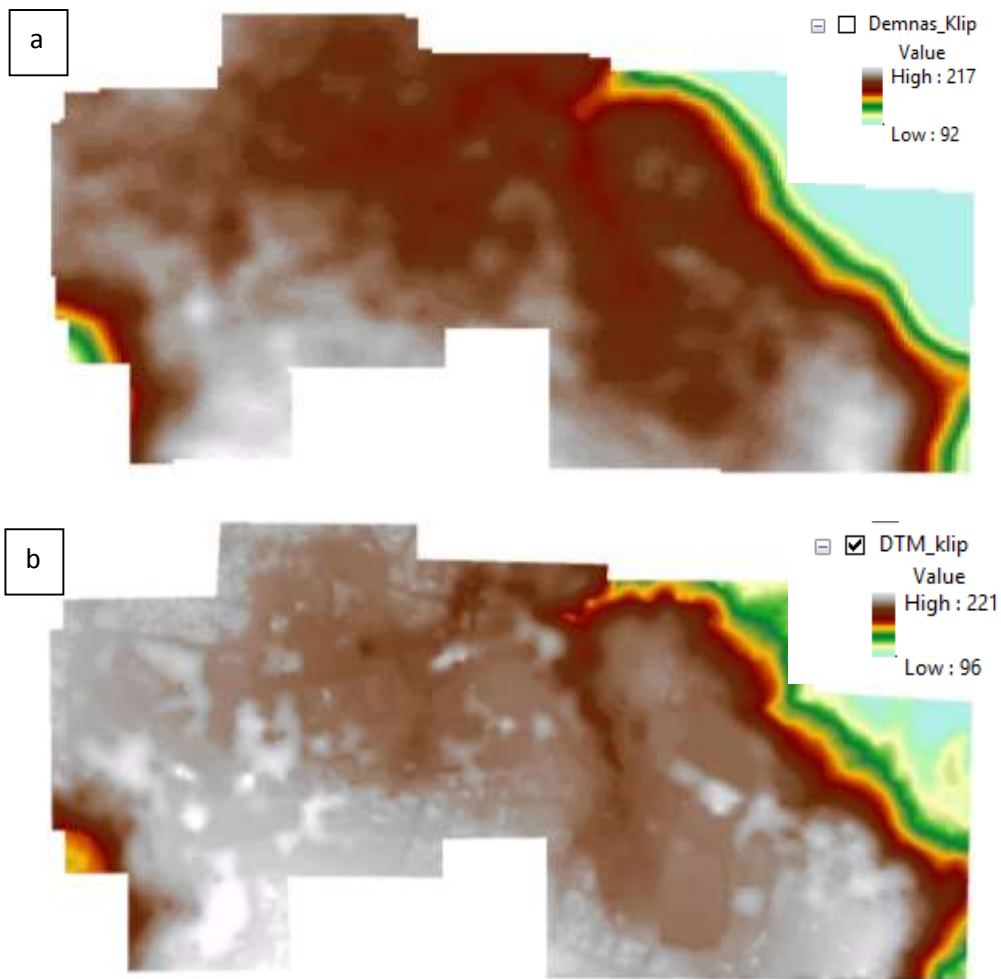


Fig. 3. DEMNAS from BIG, Indonesia (a), DEM from the drone (b)

In general, both DEM has a similar pattern although the data is not 100% the same, because of the drone somewhat less precise for areas that have a sudden slope [36] such as UNNES region. (Fig.4.) Indicates that they are a significant difference on maximum minimum data 4 m, and 1 m deviation. The amount of data is different because both have different spatial resolutions, yet both have a good correlation value. Based on Pearson coefficients and matrix of mission/commission of 0.98, which means the DSM data acquisition results reliable enough to be used in the high-resolution terrain analysis.

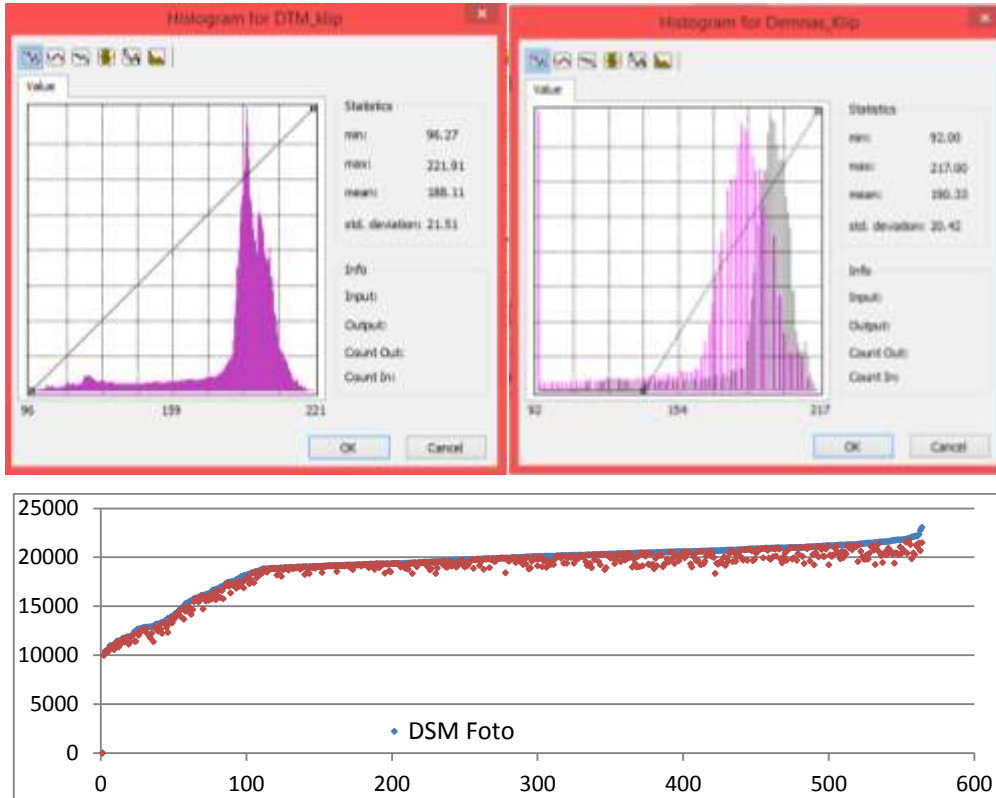


Fig.4. Histogram Deviation of DEMNAS and DSM.

Beside the reliability, the drone data also has the disadvantage that can not be avoided by a wide variety of panchromatic sensor. The disadvantage of photogrammetric system are they records what may appears on the camera as a three-dimensional form. This capability is very useful in three-dimensional modeling, but not when used for the generating elevation data either DSM or DTM. Drone data capabilities in creating DTM are dependent on processing software, because the different algorithm to separate land cover such as buildings, forests, or other solid appearance. (Fig.5.) Shows compare DSM, DTM, and DEMNAS. The transverse incision show some of the weaknesses and strengths of both DEM from DEMNAS data and drones. In the covered area in by C1 building, drone DTM results has a different pattern with DEMNAS, but in open areas such as open field (football pitch) drones showing superior results. DEMNAS results apparent generated on amount data part, it is seen with very smooth curve displacement. Different with DSM Drone is very volatile and show the more detail data. But in reality that is the drone data limits, so that it can be overcome by the correction in other software manually, but it is very subjective based on interpretation.



Fig.5. (A) Orthophoto topographic profile in FIS UNNES campus, **(b)** Profile Topography A - A'

Flow Accumulation is a summation model or accumulation of flow direction between each grid according to the dominant slope. In nature, the flow accumulation in smaller amounts would be small channel and with massive accumulation will be the river. Flow accumulation with raster data modeling can be made into a flow pattern (stream) by using limit/ threshold which assumed from minimum flow as a river or drainage[32], Threshold limit in the flow direction are used as a basis approximate UNNES to estimate the flow accumulation or basin. The threshold is very dependent on the resolution datasets[24], And topographic characteristics. **Fig.6.** Shows a comparison between the flow direction of the UNNES cluster. Dark blue color indicates a high potential inundation and light blue color shows the low potential inundation.

are small and less precise placements result in less optimal water conservation. On the UNNES area recommends the construction of recharge wells to a depth of 3 meters and 80 cm diameter with total 1,388 pieces to reducing the discharge 5.97 m³/sec [37].

4. Conclusion

The conclusion of this research is:

- Drones have the ability as a source of Topographic data by carrying out Certain requirements such as a special representative of the GCP, good quality photos and low altitude. Accuracy of the data research shows a value of 0.98 meters.
- Drone Data has the flexibility on the spatial resolution and all the needed characteristics for micro DSM morphometric and hydrological analysis. This research using RMSV RMSH 2.5 cm and 5.1 cm.
- The UNNES region has a potential for the basin for inundation on Social Science Faculty, Faculty of Economics, and Education Science Faculty, and intersection road.

References

- [1] S. Lee, S. Taemin, K. Sungjoong, P. Junwoo, H. Kyungwoo, and B. Hyochoong, "Vision-Based Autonomous Landing of a Multi- Copter Unmanned Aerial Vehicle using Reinforcement Learning," *2018 Int. Conf. Unmanned Aircr. Syst.*, pp. 108–114, 2018.
- [2] E. Akturk and A. O. Altunel, "Accuracy Assesment of a Low-Cost UAV Derived Digital Elevation Model (DEM) in a Highly Broken and Vegetated Terrain," *Measurement*, 2018.
- [3] G. Salvo, L. Caruso, and A. Scordo, "Urban traffic analysis through an UAV," *Procedia - Soc. Behav. Sci.*, vol. 111, pp. 1083–1091, 2014.
- [4] S. A. Mouloua, J. Ferraro, M. Mouloua, P. A. Hancock, and C. Florida, "Trend Analysis Of Unmanned Aerial Vehicles (UAV S) Research Published In The HFES Proceedings," pp. 1067–1071, 2018.
- [5] J. Suh and Y. Choi, "Mapping hazardous mining-induced sinkhole subsidence using unmanned aerial vehicle (drone) photogrammetry," *Environ. Earth Sci.*, 2017.
- [6] A. M. Cunliffe, R. E. Brazier, and K. Anderson, "Remote Sensing of Environment Ultra- fi ne grain landscape-scale quanti fi cation of dryland vegetation structure with drone-acquired structure-from-motion photogrammetry," *Remote Sens. Environ.*, vol. 183, pp. 129–143, 2016.
- [7] G. Sammartano and A. Spanò, "DEM Generation based on UAV Photogrammetry Data in Critical Areas DEM Generation based on UAV Photogrammetry Data in Critical Areas," no. May, 2016.
- [8] V. Moudrý *et al.*, "Comparison of a commercial and home-assembled fixed-wing UAV for terrain mapping of a post- mining site under leaf-off conditions," *Int. J. Remote Sens.*, vol. 00, no. 00, pp. 1–18, 2018.
- [9] S. H. Sadeghi, M. Moradi Dashtpaderdi, H. Moradi Rekabdarkoolai, and J. M. Schoorl, "Accuracy of sedimentgraph modeling from topography map scale and DEM mesh size," *Int. Soil Water Conserv. Res.*, vol. 7, no. 2, pp. 138–149, 2019.
- [10] O. Ridge and O. Ridge, "Spatial and temporal variability in streamflow generation on the West Fork of Walker Branch Watershed," vol. 142, no. 1993, pp. 137–166, 2008.
- [11] F. WOOD, ERIC, M. SIVAPALAN, K. BEVEN, and B. LARRY, "The influence of

catchment scale on hydrologic response and its importance in rainfall-runoff modeling has been recognized since the early 1960s (Minshall , 1960 ; Amorocho , 1961). Qualitatively it has been recognized that as the spatial scale of the c,” vol. 102, pp. 29–47, 1988.

- [12] I. Ahmad, “Digital elevation model (DEM) coupled with geographic information system (GIS): an approach towards erosion modeling of Gumara watershed , Ethiopia,” 2018.
- [13] R. Turcotte, J. Fortin, A. N. Rousseau, S. Massicotte, and J. Villeneuve, “Determination of the drainage structure of a watershed using a digital elevation model and a digital river and lake network,” vol. 240, pp. 225–242, 2001.
- [14] M. Jha, P. W. Gassman, S. Secchi, R. Gu, and J. Arnold, “Effect Of Watershed Subdivision On Swat Flow , Sediment , And Nutrient Predictions 1,” vol. 76502, pp. 811–825, 2004.
- [15] Z. Lai, S. Li, G. Lv, Z. Pan, and G. Fei, “Watershed delineation using hydrographic features and a DEM in plain river network region,” vol. 288, no. July 2015, pp. 276–288, 2016.
- [16] J. Krenz and N. J. Kuhn, *Chapter 8 - Assessing Badland Sediment Sources Using Unmanned Aerial Vehicles*. Elsevier Inc., 2018.
- [17] F. J. Aguilar, J. P. Mills, J. Delgado, M. A. Aguilar, J. G. Negreiros, and J. L. Pérez, “ISPRS Journal of Photogrammetry and Remote Sensing Modelling vertical error in LiDAR-derived digital elevation models,” *ISPRS J. Photogramm. Remote Sens.*, vol. 65, no. 1, pp. 103–110, 2010.
- [18] S. . Smith, D. . Holland, and P. . Longley, “The Importance Of Understanding Error In Lidar Digital Elevation Models,” 2001.
- [19] J. D. Giglierano, “LiDAR basics for natural resource mapping applications,” pp. 103–115, 2016.
- [20] L. T. Sze *et al.*, “High resolution DEM generation using small drone for interferometry SAR,” *Int. Conf. Sp. Sci. Commun. Iconsp.*, vol. 2015-Septe, pp. 366–369, 2015.
- [21] N. Polat and U. Murat, “An Experimental Analysis of Digital Elevation Models Generated with Lidar Data and UAV Photogrammetry,” *J. Indian Soc. Remote Sens.*, vol. 8, 2018.
- [22] W. Li, D. Han, and H. Li, “Extraction of digital terrain model based on regular mesh generation in mountainous areas,” 2017.
- [23] P. Kumar and R. Kshitij, “A GIS-based approach in drainage morphometric analysis of Kanhar River Basin , India,” *Appl. Water Sci.*, vol. 7, pp. 217–232, 2017.
- [24] H. Zhang *et al.*, “An integrated algorithm to evaluate flow direction and flow accumulation in flat regions of hydrologically corrected DEMs,” *Catena*, vol. 151, pp. 174–181, 2017.
- [25] S. Wahyuningsih, F. Usman, and L. Rohman, “Pembuatan Jaringan Sungai Dan Karakteristik Topografi Das Dari DEM- Jatim,” *MEDIA Tek. SIPIL*, vol. 8, no. 2, pp. 99–108, 2008.
- [26] K. Ramadhoni and I. Rudiarto, “Pengaruh Eksistensi Kawasan Pendidikan Unnes Terhadap Perkembangan Guna Dan Harga Lahan Di Sekaran , Kota Semarang,” *J. Tek. PWK*, vol. 3, no. 4, pp. 585–595, 2014.
- [27] S. I. Supriyadi, “Struktur Bawah Permukaan Sekaran Dan Sekitarnya Berdasarkan Data Gaya Berat,” *Unnes Phys. J.*, vol. 3, no. 1, pp. 7–13, 2014.
- [28] M. Rabah, M. Basiouny, E. Ghanem, and A. Elhadary, “Using RTK and VRS in direct geo-referencing of the UAV imagery,” *NRIAG J. Astron. Geophys.*, vol. 7, no. 2, pp.

220–226, 2018.

- [29] J. R. Parent and J. C. Volin, “Assessing the potential for leaf-off LiDAR data to model canopy closure in temperate deciduous forests,” *ISPRS J. Photogramm. Remote Sens.*, vol. 95, pp. 134–145, 2014.
- [30] A. Lucieer, D. Turner, D. H. King, and S. A. Robinson, “Using an unmanned aerial vehicle (UAV) to capture micro-topography of antarctic moss beds,” *Int. J. Appl. Earth Obs. Geoinf.*, vol. 27, no. PARTA, pp. 53–62, 2014.
- [31] X. Li, H. Shen, R. Feng, J. Li, and L. Zhang, “DEM generation from contours and a low-resolution DEM,” *ISPRS J. Photogramm. Remote Sens.*, vol. 134, pp. 135–147, 2017.
- [32] R. Jones, “Algorithms for using a DEM for mapping catchment areas of stream sediment samples,” *Comput. Geosci.*, vol. 28, pp. 1051–1060, 2002.
- [33] M. Keneddy, *The global positioning system and GIS: An introduction*, 2nd Editio. London And Newyork: Taylor & Francis, 2002.
- [34] U. Peeroo, I. Oludare, Mohammed, and V. Saeidi, “Building extraction for 3D city modelling using airborne laser scanning data and high- resolution aerial photo,” *South African J. Geomatics*, vol. 6, no. 3, pp. 363–376, 2017.
- [35] K. L. Cook, “Geomorphology An evaluation of the effectiveness of low-cost UAVs and structure from motion for geomorphic change detection,” *Geomorphology*, vol. 278, pp. 195–208, 2017.
- [36] F. Mancini, M. Dubbini, M. Gattelli, F. Stecchi, S. Fabbri, and G. Gabbianelli, “Using Unmanned Aerial Vehicles (UAV) for High-Resolution Reconstruction of Topography: The Structure from Motion Approach on Coastal Environments,” *Remote Sens.*, vol. 5, pp. 6880–6898, 2013.
- [37] B. Sugiyarto, “Kajian Jaringan Drainase Kampus UNNES Menuju Sistem Drainase Berwawasan Lingkungan,” *J. Tek. Sipil dan Perenc.*, vol. 19, no. 2, pp. 136–142, 2019.
- [38] I. Saud, “Kajian Penanggulangan Banjir di Wilayah Pematuan Surabaya Barat,” *J. Apl.*, vol. 3, no. 1, pp. 1–10, 2007.